

Method to Site-Specifically Identify and Quantitate Carbonyl End Products of Protein Oxidation Using Oxidation-Dependent Element Coded Affinity Tags (O-ECAT) and NanoLiquid Chromatography Fourier Transform Mass Spectrometry

Susan Lee,^{†,‡} Nicolas L. Young,^{†,‡,§} Paul A. Whetstone,[‡] Sarah M. Cheal,[‡] W. Henry Benner,[§] Carlito B. Lebrilla,^{*,‡} and Claude F. Meares^{*,‡}

Department of Chemistry, University of California–Davis, Davis, California, and Biosecurity and NanoSciences Laboratory, Lawrence Livermore National Laboratory, Livermore, California

Received September 6, 2005

Protein oxidation is linked to cellular stress, aging, and disease. Protein oxidations that result in reactive species are of particular interest, since these reactive oxidation products may react with other proteins or biomolecules in an unmediated and irreversible fashion, providing a potential marker for a variety of disease mechanisms. We have developed a novel system to identify and quantitate, relative to other states, the sites of oxidation on a given protein. This presents a significant advancement over current methods, combining strengths of current methods and adding the abilities to multiplex, quantitate, and probe more modified amino acids. A specially designed Oxidation-dependent carbonyl-specific Element-Coded Affinity Mass Tag (O-ECAT), AOD, ((*S*)-2-(4-(2-aminooxy)-acetamido)-benzyl)-1,4,7,10-tetraazacyclododecane-*N,N',N'',N'''*-tetraacetic acid, is used to covalently tag the residues of a protein oxidized to aldehyde or keto end products. O-ECAT can be loaded with a variety of metals, which yields the ability to generate mass pairs and multiplex multiple samples. The O-ECAT moiety also serves as a handle for identification, quantitation, and affinity purification. After proteolysis, the AOD-tagged peptides are affinity purified and analyzed by nanoLC–FTICR–MS (nanoliquid chromatography–Fourier transform ion cyclotron resonance–mass spectrometry), which provides high specificity in extracting coeluting AOD mass pairs with a unique mass difference and allows relative quantitation based on isotopic ratios. Using this methodology, we have quantified and mapped the surface oxidation sites on a model protein, recombinant human serum albumin (rHSA) in its native form (as purchased) and after FeEDTA oxidation both at the protein and amino acid levels. A variety of modified amino acid residues including lysine, arginine, proline, histidine, threonine, aspartic, and glutamic acids, were found to be oxidized to aldehyde and keto end products. The sensitivity of this methodology is shown by the number of peptides identified, twenty peptides on the native protein and twenty-nine after surface oxidation using FeEDTA and ascorbate. All identified peptides map to the surface of the HSA crystal structure, validating this method for identifying oxidized amino acids on protein surfaces. In relative quantitation experiments between FeEDTA oxidation and native protein oxidation, identified sites showed different relative propensities toward oxidation, independent of amino acid residue. This novel methodology not only has the ability to identify and quantitate oxidized proteins but also yields site-specific quantitation on a variety of individual amino acids. We expect to extend this methodology to study disease-related oxidation.

Keywords: protein oxidation • mass tag • element-coded affinity tag (ECAT) • nanoLC–FTICR–MS

Introduction

Protein oxidation has been implicated in cellular stress, aging, and disease.^{1–4} In these systems, many different types

of oxidative protein modifications, such as cysteine and methionine oxidation, nitration of tyrosine residues, or aldehyde formation from oxidation of lysine, arginine, proline, glutamic, or aspartic acids, may occur.^{1,5–7} Of particular interest are the side chain oxidations that result in reactive carbonyl groups due to their reactivity and potential deleterious effects in biological systems. Carbonyls are known protein cross-linking agents⁸ and markers for protein degradation.⁴ When cellular

* To whom correspondence should be addressed. E-mail: cblebrilla@ucdavis.edu, cfmeares@ucdavis.edu.

[†] These authors contributed equally to this work.

[‡] University of California, Davis.

[§] Lawrence Livermore National Laboratory.

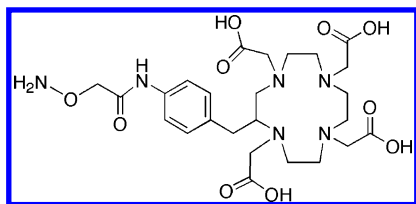


Figure 1. Oxidation-specific Element-Coded Affinity Tag (O-ECAT): AOD, (((S)-2-(4-(2-aminooxy)acetamido)-benzyl)-1,4,7,10-tetraazacyclododecane-*N,N,N',N''*-tetraacetic acid).

protein degradation pathways fail, these species may react with other biomolecules in an unmediated manner potentially forming aggregates of cross-linked biomolecules.⁸ Protein aggregation is observed as a morphological change in some oxidation linked diseases such as Alzheimer's disease.² Aldehyde and ketone groups are also particularly well-suited for use as markers of protein oxidation because they are relatively stable and present in detectable amounts in tissues.¹ They have also been shown to be the major products of metal-catalyzed oxidation of surface residues lysine and arginine.⁷

Current methods used to study protein oxidation either visualize oxidized proteins using an oxidation-dependent tag or identify oxidation sites using mass spectrometry. The most commonly used derivatization agent to detect oxidation is 2,4-dinitrophenylhydrazine (DNPH). DNPH can be used in UV studies of protein oxidation or in combination with an anti-DNPH antibody to visualize proteins using Western blotting.⁹ This results in identification of the oxidized proteins but does not give information about the specific oxidation site. The DNPH assay can also be problematic due to the poor solubility of DNPH in aqueous buffers and chromophore contamination.¹⁰

Mass spectrometry has been used to detect specific amino acid oxidation through the most common characteristic mass shifts, i.e., +16 Da.^{5,6,11} This methodology has been shown to be useful for individual amino acids, peptides, and small proteins but has not been utilized with larger proteins. Concern about direct detection methods exist due to potential oxidation from processing¹² and the electrochemical nature of some ion sources such as electrospray. It is important to note that the oxidative changes seen in direct detection are often reversible changes, i.e., methionine oxidation, not the stable aldehyde and ketone oxidation end-products studied here.

Recently, there have been some examples of using an oxidation-specific tag to label protein carbonyl groups and/or to identify the modification sites by mass spectrometry.^{13–15} In these experiments, biotin hydrazide was used to tag the oxidized protein. There was some nonspecific binding of the hydrazide to the protein¹³ and the endogenous biotinylation within cells can also be an issue.¹⁵

Here, we present the development of a single method to visualize, quantitate, and site-specifically identify aldehyde and ketone oxidation sites on protein surfaces using an oxidation-dependent carbonyl-specific element-coded affinity tag (O-ECAT), ((S)-2-(4-(2-aminooxy)acetamido)-benzyl)-DOTA (AOD, Figure 1) in conjugation with nanoLC-FTICR-MS (nanoLiquid Chromatography Fourier Transform Ion Cyclotron Resonance Mass Spectrometry). AOD has two key elements: 1) an aminoxy group that can form a covalent bond with aldehydes or ketones, and 2) a DOTA (1,4,7,10-tetraazacyclododecane-*N,N,N',N''*-tetraacetic acid) metal-chelator moiety. AOD is water soluble and can be loaded with a wide choice of monoisotopic rare earths to generate a series of mass tags with

large mass defects¹⁶ and nearly identical chromatographic behavior.¹⁷ Confirmation of the labeling is achieved using Western blotting. Competitive ELISA is used to quantitate the AOD chelates per protein.¹⁹ The protein is then digested with trypsin. Affinity purification is achieved using an immobilized antibody to M-DOTA, 2D12.5.^{17,18} Identification and quantitation of the AOD-peptides are achieved through the unique mass signatures and elemental ratios observed by nanoLC-FTICR-MS. An algorithm is applied to the data that extracts the tagged peptides based on coelution of the mass tags. Comparison of the observed masses to an in silico digest identifies the specific site of oxidation. This presents a significant advancement over current methods, combining strengths of current methods and adding the abilities to multiplex, quantitate, and probe more modified amino acids. In this paper, the oxidation sites of recombinant human serum albumin (rHSA), both in its native form and after FeEDTA (iron (III) ethylenediaminetetraacetic acid)-induced oxidation, are mapped onto an HSA crystal structure (PDB file: 1AO6, www.rcsb.org)²⁰ as proof of concept. A variety of modified residues were identified and all map onto the surface of the protein. The methodology has also been used for site-specific quantitation between the two above samples. The quantitative results showed significant increase in oxidation between sites.

By studying the nature of protein oxidation on the site-specific level we hope to further the understanding of the mechanisms of oxidation related diseases and the role of free radical oxidation in biology.

Experimental Section

Materials. Recombinant human serum albumin, rare earth hexahydrate salts, and *p*-nitrophenyl phosphate were purchased from Sigma Aldrich (St. Louis, MO). The DOTA derivative, AOD was synthesized as described below. The anti-M-DOTA antibody 2D12.5 was a generous gift from Dr. David Goodwin, Palo Alto Veterans Administration Hospital (Palo Alto, CA). Goat anti-mouse lambda IgG-alkaline phosphatase conjugate was purchased from Southern Biotechnology (Birmingham, IL). Modified sequencing grade trypsin was purchased from Promega (Madison, WI). BCA reagents and aminolink plus resin were purchased from Pierce (Rockford, IL). 96-well plates were obtained from Fisher Scientific. Pure water (18MΩ cm) was used throughout.

Chelate Synthesis. (S)-2-(4-aminobenzyl)-DOTA tetra-tert-butyl ester, ABD-*t*Bu₄, was synthesized as described previously.^{21–23} ¹H NMR (300 MHz, CDCl₃) δ 1.0–4.0 (m, 63H), 6.39 (d, *J* = 8.7 Hz, 2H), 6.73 (d, *J* = 8.7 Hz, 2H). ESI-MS: calculated (M+H)⁺ *m/z* 734.51, observed 734.50.

(S)-2-(4-(2-aminooxy)acetamidobenzyl)-1, 4, 7, 10-tetraazacyclododecane-*N,N,N',N''*-tetraacetic acid (AOD). 2.60 g *N*-Boc-aminoxyacetic acid was dissolved in a minimal volume of *N,N*-dimethylformamide (DMF) and brought to a final volume of 50 mL with CH₂Cl₂. The solution was cooled in an ice bath to 0 °C, and 1.04 mL of diisopropylcarbodiimide (DIPCDI) was added with stirring. After 30 min, the solvent was removed under vacuum and a solution of 1.00 g ABD-*t*Bu₄ dissolved in 20 mL DMF supplemented with 0.5 mL diisopropylethylamine was added at RT. The solution was stirred for 2 h, after which 200 mL of a 1% solution of triethylamine (TEA) in water was added, and then extracted 5× with 20 mL aliquots of ethyl acetate. The organic fractions were combined, dried over sodium sulfate and brought to dryness under vacuum, providing (S)-2-(4-(2-*N*-Boc-aminoxy)acetamido-benzyl)-1,4,7,10-tetraazacyclododecane-*N,N,N',N''*-tetraacetic acid tetra-

tertbutyl ester in quantitative yield. The product was dissolved in neat trifluoroacetic acid and stirred overnight under a light stream of nitrogen. The resulting light yellow oil was dissolved in water and lyophilized to give AOD in quantitative yield as a flocculent white solid. HPLC analysis of the product by UV absorbance at 280 nm indicated greater than 98% purity. ^1H NMR (300 MHz, $\text{C}_2\text{D}_6\text{SO}$) δ 1.0–4.0 (m, 27H), 4.16 (s, 2H), 7.23 (d, $J = 8.1$ Hz, 2H), 7.65 (d, $J = 8.1$ Hz, 2H), 8.31 (s, 2H), 9.69 (s, 4H). ESI-MS: calculated $(\text{M}+\text{H})^+ m/z$ 583.27, observed 583.26.

Metalation. AOD was metalated by combining the chelate with 1.8 equivalents of M-Cl_3 , 35 mM and 59 mM respectively, in 0.1 M ammonium acetate, pH 6.1 for 2 h at 37 °C before 1.8 equiv. of diethylenetriamine- N,N,N',N'',N''' -pentaacetic acid (DTPA) were added to completely scavenge any excess metal. Complete metalation was confirmed by LC–MS and the chelates were used without further purification.

Protein Oxidation. rHSA (592 μM aliquots) dialyzed into cleavage buffer [10 mM MOPS, 120 mM NaCl, 10 mM MgCl_2 , 1 mM EDTA, pH 7.9], was oxidized with 20 mM iron (III) EDTA (FeEDTA) and 20 mM ascorbate while the native controls had no oxidants added. The oxidation reaction was mixed and allowed to proceed at RT for 15 min before being dialyzed into tagging buffer [100 mM KH_2PO_4 , 0.5 M NaCl, pH 6.5]. Oxidation conditions were designed to minimize protein backbone cleavage and maintain structural integrity of the protein. Western blotting confirmed these parameters (data not shown).

AOD Labeling. Native and oxidized rHSA were labeled overnight at RT with two different M-AOD, e.g., Tb and Ho, while one aliquot of native rHSA was processed in parallel with no added M-AOD. The reactions were then extensively dialyzed into 50 mM HEPES, pH 7.5. Protein concentration was determined using the Pierce microBCA method. Aliquots were taken for the gels, blots, and ELISA before the remaining protein was reduced, alkylated with iodoacetamide, and trypsin digested. To achieve site-specific quantitation, the same procedure was used except one M-AOD aliquot from FeEDTA/ascorbate-oxidized rHSA was combined with a different M-AOD aliquot of native rHSA control after trypsin digestion.

To confirm that the tags were incorporated into the protein, samples were loaded onto duplicate Invitrogen 10–20% Tris-glycine gels and were run for 1.5 h at 125 V in Laemmli buffer [25 mM Tris, 192 mM glycine, 0.1% SDS]. One gel was stained using SYPRO Ruby and imaged using the ChemXRS imager (Biorad). The duplicate gel was blotted onto a PDVF membrane in CAPS buffer [10 mM CAPS, 10% methanol] for 1.5 h at 50 V. The blot was then blocked with 5% nonfat milk in TBS [24.8 mM Tris, 137 mM NaCl, 0.269 mM KCl, pH 7.4] overnight. The blot was rinsed 4 \times with TBST [TBS with 0.05% (v/v) Tween-20]. A 1:5000 dilution of the 1 mg/mL anti-M-DOTA antibody 2D12.5 in TBST was added to the blot and allowed to incubate for 1 h at RT with vigorous mixing. The blot was then rinsed 4 \times with TBST and a 1:2000 dilution of the secondary antibody in TBST, a goat anti-mouse lambda-AP conjugate, was added and allowed to incubate at RT for 1 h with vigorous mixing. The blot was then rinsed 3 \times with TBST and 1 \times with TBS before being developed with BCIP/NBT in 0.1 M Tris pH 9.5, 0.5 mM MgCl_2 . The Western blot was visualized using an HP5490c scanner.

Competitive ELISA. A competitive ELISA was used to quantitate the tagging yield.¹⁹ First, clear, high-binding plates were coated with 0.3 pmol of HSA-2-iminothiolane-Y-((S)-2-(4-(2-bromo)-acetamido)-benzyl)-DOTA in 50 mM Na_2CO_3 (pH 9.6) and stored at 4 °C overnight. Wells were emptied and rinsed 3 \times with TBST. The wells were then blocked with 200 μL of 1% bovine serum albumin in TBS, at 37 °C for 2 h. A total of

25 μL of competitor M-(S)-2-(4-nitrobenzyl)-DOTA (M-NBD) or 25 μL of the AOD-tagged protein, from concentrations of micromolar to femtomolar, was then added to the wells with 25 μL of 2 nM anti-M-DOTA antibody 2D12.5. Each sample was done in triplicate and run on the same plate. The plate was incubated at RT for 1 h with mixing. The wells were rinsed 3 \times with TBST and then 50 μL of 1:4000 dilution of goat anti-mouse lambda-AP was added to all wells. The plate was again incubated at RT for 1 h with mixing. The plate was rinsed 3 \times with TBST and 1 \times with 10 mM diethanolamine, 0.5 mM MgCl_2 , pH 9.5. 200 μL of a 1 mg/mL solution of *p*-nitrophenyl phosphate in the diethanolamine solution was then added to the wells. The plate was read at 405 nm for 30 min at RT, using a kinetic reading every minute.

Trypsin Digestion. The trypsin protocol was as follows: (1) denature and reduce protein with 5 M urea, 0.125 M HEPES, pH 7.5, 28 mM DTT (dithiothreitol) for 45 min at 37 °C; (2) alkylate the cysteines by adding iodoacetamide to a final concentration of 56 mM and incubating at RT for 20 min in the dark; (3) reduce the concentration of the urea to 1 M using 50 mM HEPES, pH 7.5, and add CaCl_2 to a final concentration of 1 mM; (4) add sequencing grade modified trypsin (1:50 wt: wt ratio) and incubate at 37 °C overnight.

Affinity Purification of AOD Peptides. The 2D12.5 antibody was coupled to Pierce aminolink plus resin and used for the affinity purification, essentially as described.¹⁷ Briefly, after the trypsin digestion, the two M-AOD sets for each sample were combined and loaded onto 200 μL 2D12.5 aminolink resin that had been equilibrated with loading buffer [25 mM triethylammonium acetate (TEAOAc), pH 7]. The column was then washed with 12 column volumes (CVs) each of (1) loading buffer, (2) loading buffer + 1M NaCl, pH 7, (3) 0.5% acetic acid, pH 2.8, (4) 4 M urea, and (5) 1 \times loading + 20% acetonitrile with 2 CVs loading buffer wash between all the washes. The tagged peptides were then eluted with 20 CVs of 50% acetonitrile/0.4% trifluoroacetic acid. Elution fractions were combined and dried using a speed-vac.

NanoLC–FTICR–MS Instrumentation. The nanoliquid chromatography pumps used in this work were the first prototype of a pump and a 2D-nanoLC system developed by Eksigent Technologies (Livermore, CA). The development of the nanoLC–FTICR–MS platform for this analysis is the first implementation of an LC–MS system based on this technology. The nanospray tips were produced in-house from 75 μm ID fused silica tubing using a Sutter Instruments Co. Model P2000 laser tip puller. The chromatographic stationary phase of 5 μm Luna C18 (Phenomenex) was packed directly into the nanospray tip by bomb loading a slurry in 70% ethanol such that the nanospray tip and the chromatographic column are integrated with the column terminating at the approximately 15 μm diameter nanospray tip.

The mass spectrometer is a 9.4 T Apex II Fourier Transform Ion Cyclotron Resonance Mass Spectrometer (Bruker, Waltham, MA) with a modified Apollo source. Only part of the Apollo source is used in the nanospray configuration. The drying gas heater has been modified to deliver drying gas temperatures up to about 400 °C and is operated at 350 °C here. The main purpose of this gas is to heat the glass capillary which serves as the vacuum interface to the mass spectrometer. The nanospray interface is a home-built system with the pulled glass capillary kept at ground potential through a liquid junction of a platinum wire with the solvent in a low dead-volume tee. The nanospray potential of approximately 2 kV is delivered to the counter-electrode/sampling orifice of the mass spectrometer. On the original Apollo electrospray source the sampling

orifice was on a flat surface and was approximately 0.5 mm in diameter. This has been modified such that the nanospray tip sees an approximately 3 mm entrance that is later reduced to 0.5 mm. The primary potential that the nanospray tip sees is from an inverted cone that extends from the 3 mm orifice at a slightly obtuse angle. The nanospray tip is placed on-axis approximately 1 cm from the 0.5 mm orifice. This geometry allows for two important effects. The ions are forced to traverse a distance of approximately 1 cm of atmospheric pressure, effectively desolvating the ions, yet are also effectively entrained in the directed fluid dynamic flow into the mass spectrometer. Significant improvements in sensitivity and stability have been realized from this modification as this work progressed.

NanoLC–FTICR–MS Analysis. The AOD-tagged, digested, and affinity purified samples were analyzed by reversed phase nanoliquid chromatography-Fourier transform ion cyclotron resonance mass spectrometry (nanoLC–FTICR–MS) using the instrument described above. Affinity elutions from the 2D12.5 column were loaded onto an approximately 10 cm long 75 μ m ID in-house packed C18 column. The gradient of A (10 mM ammonium acetate, 0.1% formic) to B (0.1% formic in 90% acetonitrile) was from 10 to 50% B over 55 min. Column effluent was directly interfaced with a home-built nanospray source into a Bruker Apex II 9.4T FTMS which collected data from 450 to 2000 m/z . Six 256k transients were co-added every 0.1 min without quenching the accumulation hexapole between acquisitions resulting in nearly 100% duty cycle. Spectra were acquired in broadband mode without internal mass calibration or software-based correction for space charging effects.

Data Analysis. To simplify the analysis, the mass spectral information was processed using in-house software based on isotopic mass differences to give [M+H]⁺ ion masses. The spectra were zero-filled once and apodized before fast Fourier transformation and data processing. The masses of the tagged peptides were extracted from the data based on the characteristic mass difference between the two metal-AOD tags and coelution of the tagged mass pairs. The coelution of the mass pairs simplifies the data analysis and provides more robust quantitation.²⁴ The tagged peptide masses were then compared to an in silico rHSA digest allowing for up to two missed cleavages, with variable cysteine alkylation, and adjustments for the possible oxidation and tagging modifications. For example, oxidized lysine results in an amino adipic semialdehyde,⁷ which has only one amu difference from the non-oxidized form, M-1. But the oxidized lysine tagged with TbAOD forms a specifically tagged lysine which has a mass difference of over 700 from the non-oxidized form, M+719. The unique mass tags from oxidized lysine, arginine, proline, threonine, histidine, and glutamic and aspartic acids were considered.^{5–7,25} Using TbAOD, the modified masses would be M+719, 677, 736, 718, 668, 690, and 690, respectively. Since the mass difference for glutamic and aspartic acids are the same, these residues are not distinguished in this methodology. See Table 1A,B for peptide examples. For relative quantitation experiments, the transients for each coeluting pair of masses were summed across the chromatographic peak before apodization and Fourier transformation. Relative quantitation was determined by a ratio of peak heights between the two metal-AOD peaks using the tallest peak in each isotopic cluster.

Results and Discussion

AOD Labeling. Although the natural genetic code does not include aldehyde or ketone-containing amino acids, proteins generally exhibit some level of aldehyde or ketone content even

in the absence of purposeful oxidation.^{10,11,26,27} One of the many advantages of the O-ECAT AOD system is the availability of the 2D12.5 monoclonal antibody specific for a range of M-DOTA chelates.¹⁹ This antibody was first used to confirm the covalent tagging of the protein by running a Western blot of the AOD-tagged proteins (Figure 2). There were two types of samples analyzed. The first type was rHSA (recombinant human serum albumin) as purchased from Sigma, without additional processing or oxidation. Oxidations observed in this sample are residual from production or unintentional. These samples will be referred to as “control rHSA” or “control samples.” The second sample type analyzed was rHSA purchased from Sigma and then oxidized with FeEDTA and ascorbate as described above. This sample will be referred to as “FeEDTA and ascorbate oxidized rHSA” or “FeEDTA and ascorbate oxidized samples.” In Figure 2 lane 1, rHSA with no added AOD tag shows no reactivity while both the tagged control samples and the tagged FeEDTA and ascorbate oxidized samples show distinct bands at the correct molecular weight for human serum albumin (~66kD). The oxidized protein samples show an increased intensity of labeling versus the native control lanes, as expected. Note that the metal within the AOD does not affect the labeling efficiency as seen by the equal intensity Western bands. This is further confirmed by quantitative ELISA and peptide integration of the LC–MS data (data not shown).

The 2D12.5 antibody was then used to quantify the tagging yield of the M-AOD on both the control and FeEDTA and ascorbate oxidized protein samples using the competitive ELISA (Figure 3).¹⁹ Each sample was done in triplicate and the logEC₅₀ values of the protein curves were compared with the standard TbNBD curve. Figure 3 shows that the control sample had 1 in 16 proteins was labeled with M-AOD and the FeEDTA/ascorbate oxidized sample had 1 in 9 proteins labeled, with the error bars showing one standard deviation. The untagged rHSA control (data not shown) showed no DOTA competition. The oxidation with FeEDTA and ascorbate increased the tagging yield by nearly 2-fold. A similar 2-fold increase in oxidation was also seen in human albumin oxidized with hydrogen peroxide and quantified with the DNPH blot method.⁹

Identification of the Tagged Peptides. A number of factors aid in the identification of the tagged peptides: (1) the M-AOD adds a mass tag with a large mass defect onto the modified peptide; (2) the specific reactivity of our tagging system for carbonyl-containing oxidation products; (3) the 2D12.5 monoclonal antibody affinity purification reduces the background of nonspecific peptides; (4) the high chromatographic resolution of the reversed-phase nanoLC separation requires coelution of mass pairs; and (5) and the high mass resolution of the FTICR requires those mass pairs to meet the criteria defined by (1) above. The range of possible elemental compositions is dramatically reduced beyond a typical proteomic analysis or the direct LC–MS detection of oxidized peptides. In a direct detection method it is necessary to distinguish between an oxidized peptide and an unoxidized peptide or even a completely unexpected species or impurity. The direct detection method also does not indicate at what point the oxidation occurred, if it was present initially or resulted during sample processing. In our analysis, the tagging occurs at the beginning of the sample process and is specific for oxidized amino acids. Once the oxidized sites are tagged, the O-ECAT moiety serves as a handle throughout subsequent processing: (1) as a tag for detection in Western blotting and ELISA, (2) an affinity handle for purification, and (3) a mass tag for peptide identification. The mass defect of the O-ECAT peptides separates

Table 1. Oxidized Peptides Labeled with Tb-AOD Identified on Native rHSA and on FeEDTA/Ascorbate-Oxidized rHSA^a

sequence	modified AA	sequence no.	in control?	theoretical MW	observed MW	error (ppm)
A. Native rHSA						
(K)AAC*LLPKLDELREDEGK	Lys	175–190		2547.0878	2547.0575	12
(K)ATKEQLK	Lys	539–545		1536.6024	1536.5821	13
(K)C*ASLQKFGGER	Lys	200–209		1914.7134	1914.6824	16
(K)ERQIKK	Arg	520–525		1478.5970	1478.5774	13
(K)FGERAFK	Arg	206–212		1531.5548	1531.5360	12
(R)FKDLGGEENFK	Lys	11–20		1945.7297	1945.6992	16
(R)FPKAEFAEVSK	Lys	223–233		1971.7818	1971.7495	16
(K)HPEAKR	Lys	440–445		1456.5299	1456.5101	14
(R)LAITYETTLEK	Lys	349–359		2015.8291	2015.7980	15
(K)LDELREDEGK	Asp/Glu	182–190		1764.6882	1764.6629	14
(K)LDELREDEGK	Arg	182–190		1751.6454	1751.6189	15
(K)LDELREDEGKASSAK	Lys	182–195		2237.9004	2237.8540	21
(R)LKCASLQK	Lys	198–205		1609.6374	1609.5969	25
(K)LKECCEKPLLEK	Lys	275–286		2265.9213	2265.8770	20
(K)LVNEVTEFAK	Glu	42–51		1839.7607	1839.7334	15
(R)QIKK	Lys	522–525		1235.4750	1235.4582	14
(K)SEVAHRFK	Arg	5–12		1650.6243	1650.6003	15
(K)TPVSDRVTK	Arg	467–475		1679.6607	1679.6368	14
(K)TYETTLEK	Glu	352–359		1674.6341	1674.6096	15
(K)YIC*ENQDSISSK	Asp/Glu	263–274		2133.7877	2133.7462	19
B. FeEDTA/Ascorbate-Oxidized rHSA						
(K)ADDKETCFAEEGK	Asp/Glu	561–573		2189.7775	2189.7574	9
(K)AEFAEVSK	Asp/Glu	226–233		1570.5867	1570.5804	4
(K)ATKEQLK	Lys	539–545	Y	1536.6024	1536.5913	7
(K)AVMDDFAAFVEK	Asp/Glu	546–557		2032.7804	2032.7904	–5
(K)C*ASLQKFGGER	Lys	200–209	Y	1914.7134	1914.7061	4
(K)C*AAADPHEC*YAK	Asp/Glu	360–372		2242.7439	2242.7130	14
(K)DDNPNLPR	Pro	107–114		1676.5992	1676.5863	8
(K)ECCEKPLLEK	Asp/Glu	277–286		1995.7634	1995.7441	10
(K)ETC*FAEEGKK	Thr	565–574		1902.6657	1902.6537	6
(K)ETCFAEEGK	Thr	565–573		1717.5493	1717.5282	12
(R)ETYGEMADCCAK	Asp/Glu	82–93		2124.6791	2124.6572	10
(R)ETYGEMADC*C*AKQEPER	Lys	82–98		2792.9556	2792.9229	12
(K)FGERAFK	Arg	206–211	Y	1531.5548	1531.5506	3
(R)FKDLGGEENFK	Lys	11–20	Y	1945.7297	1945.7292	0.3
(R)FPKAEFAEVSK	Lys	223–233	Y	1971.7818	1971.7767	3
(K)HKPK	His	535–538		1177.4331	1177.4288	4
(R)LAITYETTLEK	Lys	349–359	Y	2015.8291	2015.8243	2
(K)LDELREDEGK	Arg	182–190	Y	1751.6454	1751.6360	5
(K)LKECCEKPLLEK	Lys	275–286	Y	2265.9213	2265.9095	5
(K)LVNEVTEFAK	Asp/Glu	42–51	Y	1839.7607	1839.7554	3
(R)NECFLQHK	Asp/Glu	99–106		1708.6232	1708.6457	–13
(K)QEPERNEC*FLQHK	Arg	94–106		2391.8994	2391.8819	7
(K)QTALVELVK	Thr	526–534		1704.7286	1704.7038	15
(K)TPVSDR	Pro	467–472		1410.4977	1410.4861	8
(K)TPVSDRVTK	Arg	467–475	Y	1679.6607	1679.6490	7
(K)TYETTLEK	Asp/Glu	352–359	Y	1674.6341	1674.6219	7
(K)VFDEFKPLVEEPQNLK	Asp/Glu	373–389		2735.2410	2735.21111	11
(K)VHTEC*C*HGDLLCADDR	Asp/Glu	241–257		2776.9832	2776.9671	6
(K)YIC*ENQDSISSK	Asp/Glu	263–274	Y	2133.7877	2133.7689	9
(K)YIC*ENQDSISSK	Lys	263–276		2403.9456	2403.9326	5

^a The sequence of the identified peptide, along with the preceding amino acid residue, is listed with the oxidized, tagged residue indicated in bold while alkylated cysteines are indicated with asterisks. For peptides with more than one possible modified amino acid, all candidate amino acids are shown in bold.

them from any background peptides. Furthermore, our use of paired O-ECAT peptides yields another level of discrimination for the oxidized, tagged peptides.

In this proof of principle application, we have chosen to limit the scope of our work to a more easily understood system both to have a simple development platform and to understand some of the fundamentals of protein oxidation chemistry that are not yet well understood. This allows greater confidence in our results. In future work, as the complexity of the system increases, other protein fractionation steps may be needed. Since our methodology involves covalent tagging of the oxidation sites as the initial step, any low-level oxidation during subsequent steps is not a concern. Also, the means to increase confidence in assignment such as tandem mass spectrometry

or the use of internal mass standards with dual spray sources are well established.

Example LC–MS spectra are shown in Figure 4A–D. Figure 4, parts A and C, show portions of the two-dimensional plots of retention time versus m/z for the rHSA sample and the FeEDTA and ascorbate oxidized sample tagged with Tb/HoAOD, respectively. Notice that the sensitivity of this method yields complex plots showing both tagged peptides and untagged peptide contaminants. The tagged peptides can be easily distinguished from the background by observing the identical peptides tagged by the Tb/HoAOD system—see the coeluting mass pairs as seen in Figure 4B. Figure 4D displays a representative mass spectrum for a Tb/Ho mass pair. As mentioned above the rare earths contain a mass defect that distinguishes

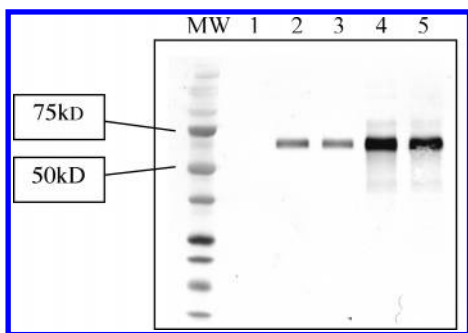


Figure 2. Western blot confirmation of the M-AOD tagging of native and FeEDTA/ascorbate oxidized rHSA. Lane 1: rHSA, lane 2: rHSA TbAOD, lane 3: rHSA HoAOD, lanes 4 & 5: rHSA oxidized with FeEDTA and ascorbate, TbAOD and HoAOD, respectively. Equal amounts of rHSA were loaded into lanes 1–5.

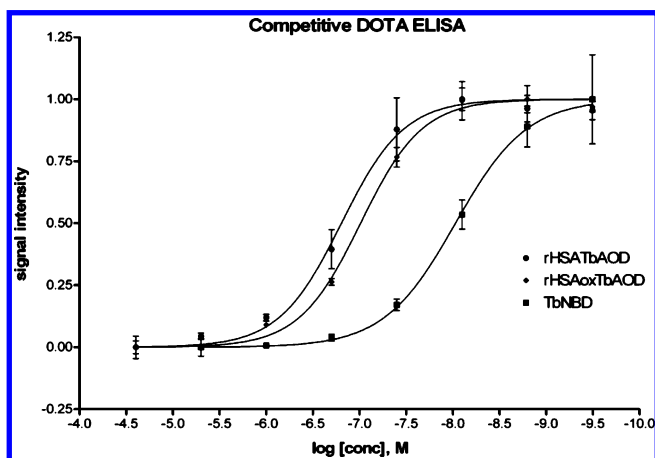


Figure 3. Competitive DOTA ELISA quantifying the tagging yield on the control rHSA TbAOD and the rHSA oxidized with FeEDTA and ascorbate, rHSAoxTbAOD. The concentration on the horizontal axis represents the log of either protein concentration (mol/L) or competitor TbNBD concentration (mol/L). Each data set was done in triplicate with the error bars showing one standard deviation.

the M-AOD peptides from background peptides; this mass defect is readily detected within the resolution of the FTICR.¹⁶ The mass of Tb is 158.925 Da while Ho has a mass of 164.930 Da, yielding a mass difference of 6.005 Da. The experimental deviation in this mass difference between the coeluting pairs has been limited to 0.02 Da, while the experimental masses for the Tb/HoAOD pairs presented here are within 0.05 Da of the theoretical masses, providing convincing resolution of the tagged peptides. These mass filters were experimentally determined by comparing error from multiple data sets (data not shown). A comparison of the isotopic distribution of the coeluting peptide-tag pair allows identification of the charge state and the high-resolution masses for the parent peptides. In Figure 4D, the m/z difference between isotopes of 0.5 and between the isotopic clusters of 3 indicate that the tagged peptides are in the +2 charge state. This spectrum was found to correspond to the TPVSDRVTK peptide where the arginine has been oxidized and tagged with M-AOD. Using this method, 20 tryptic peptides were identified in the control sample and 29 tryptic peptides (including 12 of the 20 control peptides) were identified in the FeEDTA/ascorbate oxidized sample (see Table 1A,B). Note that no peptides were identified when M-AOD was omitted from the rHSA sample (data not shown),

displaying the specificity of the tagged peptide identification. Some of the control peptides may not have been detected in the FeEDTA/ascorbate sample due to dynamic range limitations in the LC–MS analysis. High abundance peptides may mask the signal from lower abundance peptides. This is analogous to the sequence coverage differences seen between multiple LC–MS/MS runs of the same sample. Mixing one metal AOD from the control and one metal from the experiment, i.e., the relative quantitation experiments, is a more rigorous comparison of two sample sets. This eliminates concerns about the errors generated through sample handling. It also minimizes errors accumulated during MS acquisition. As can be seen in Table 1A,B, there is a systematic error in the external calibration used, which can vary across samples.

A variety of residues, including lysine, arginine, proline, histidine, threonine, and aspartic and glutamic acids, were found to be oxidized and tagged with this method. Also, all of the peptides are true tryptic peptides, displaying cleavage at lysine or arginine residues. Notice that the presence of the M-AOD on a lysine or arginine results in a missed trypsin cleavage site at that residue. A majority of the oxidized amino acids in the native protein are either lysine or arginine. These are common amino acids and their oxidation products have been seen both in radiolytic oxidation of peptides⁵ and in metal catalyzed oxidation of proteins.⁷ Since the human serum albumin used in this study is a recombinant protein, it may have been oxidized in processing. We made every effort to minimize oxidation of control samples during our work. Trace metal contamination was minimized by using high concentrations of EDTA in the reaction buffers. Even when the rHSA is pretreated with an excess of another aminoxy derivative, aminoxyacetic acid, the oxidation on the native protein is still detectable with the M-AOD system (data not shown). Robinson et al. showed that albumins from bovine, egg, and human all have background carbonyl reactivity to DNPH.⁹ Background protein oxidation has been seen in a variety of proteins, commercially available ones and those expressed in our lab, and detected with both DNPH and our M-AOD system.

The methodology was validated by mapping the oxidation sites on an HSA crystal structure, 1AO6²⁰ in Figure 5A,B. The crystals for this structure were grown from pooled HSA and from HSA expressed in *Pichia pastoris*. Both sources yielded essentially the same triclinic structure, at a resolution of 2.5 Å. In this structure, the protein is approximately 80 × 80 × 30 Å. Note that both termini, residues 1–4 and 583–585 did not have clear electron density. For the recombinant serum albumin (Sigma) used in this work, the first residue at the N-terminus, aspartic acid, was removed during expression. The oxidized amino acids are shown in red for definitively oxidized amino acids and in orange for those peptides with more than one candidate amino acid. The N-terminus is colored blue for reference. As expected, the modified oxidized residues map onto the surface of the protein. Also, more oxidized and M-AOD tagged peptides were observed in the FeEDTA/ascorbate oxidized sample. The oxidized amino acids appear to be randomly distributed on the protein surface.

Out of the 20 peptides identified within the native rHSA sample, three contain oxidized amino acids within the LDEL-RDEGK sequence (residues 182–190). This sequence was found to be oxidized and tagged at the aspartic or glutamic acid, the arginine, and the lysine residues. Examination of the crystal structure of HSA²⁰ reveals that these residues occur in the center of the protein in the bottom cleft as shown in Figure 5A, right panel. For reference, this peptide is labeled in Figure 6, right panel. This position is not known to be a metal-binding

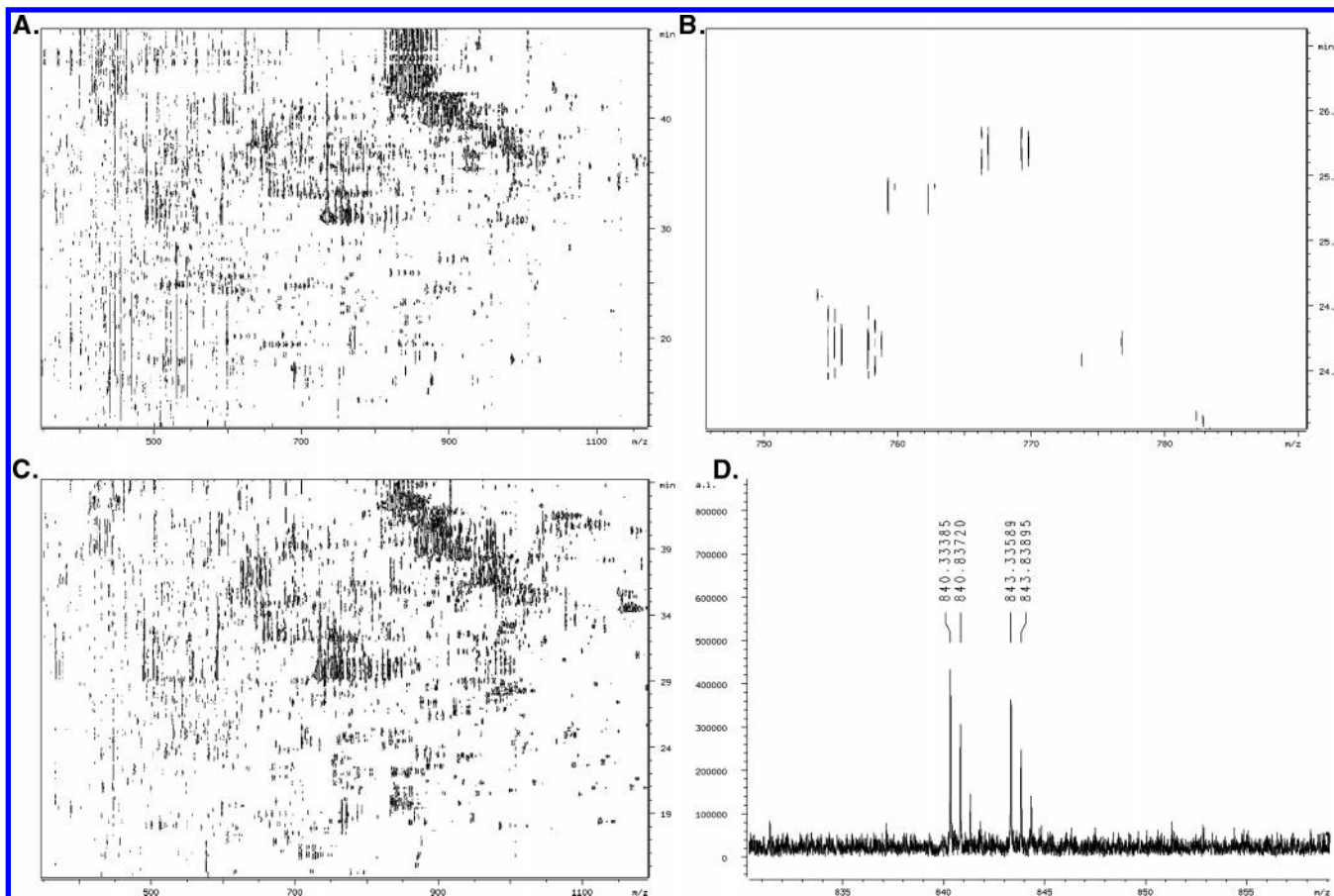


Figure 4. LC-MS spectra showing the coeluting M-AOD tagged peptide pairs. **A.** A representative portion of the two-dimensional spectrum showing m/z versus retention time for an affinity-purified rHSA sample tagged with TbAOD and HoAOD. **B.** An enlargement of the two-dimensional spectrum showing m/z versus retention time for an affinity-purified rHSA sample tagged with TbAOD and HoAOD from Figure 4A. **C.** A representative portion of the two-dimensional spectrum showing m/z versus retention time for an affinity-purified FeEDTA/ascorbate oxidized rHSA sample tagged with TbAOD and HoAOD. **D.** FTMS spectrum showing a doubly charged mass pair. The peaks shown here correspond to the peptide, TPVSDRVTK, with the arginine oxidized and tagged with TbAOD and HoAOD.

site on albumin but albumin does have multiple metal-binding sites. Albumin is known to bind metal at its N-terminus and also at a position bridging His67 and His247.²⁸ Only the oxidized arginine product of LDELRDEGK is seen in the FeEDTA/ascorbate oxidized sample.

In the FeEDTA/ascorbate sample, a larger variety of oxidized amino acids are seen. This sample also has a peptide that contains multiple oxidized amino acids, TPVSDRVTK (residues 467–475), with the oxidized arginine seen in both the native and FeEDTA/ascorbate samples while the oxidized proline product was only seen in the FeEDTA/ascorbate sample. This peptide is also not in proximity to the reported metal-binding sites on HSA. It is located on the back of the protein, near the top (Figure 5B, right panel). For reference, this peptide is labeled in Figure 6, right panel. Note that one oxidized amino acid residue, Thr566, is seen in two nested peptides, as (K)-ETC*FAEEGKK and (K)ETCFAEEGKK with the asterisk indicating an alkylated cysteine residue.

Site-Specific Quantitation of Peptides. Relative quantitation of FeEDTA/ascorbate-oxidized rHSA versus rHSA control was achieved in two parallel experiments using TbAOD and TmAOD tags. In the first experiment, TbAOD was used exclusively in tagging the FeEDTA/ascorbate-oxidized rHSA oxidation sites and TmAOD was used exclusively to tag the control rHSA oxidation sites. These samples were then mixed for relative

quantitation analysis. An identical experiment was run in parallel with the metal tags reversed, i.e., the TmAOD tag was used to tag the FeEDTA/ascorbate-oxidized rHSA oxidation sites and TbAOD was used to tag the control rHSA oxidation sites. The results of these experiments are presented in Table 2. These results share the same limitations that other peptide quantitation techniques, such as isotope-coded affinity tags (ICAT) and stable isotope labeling by amino acids in cell culture (SILAC), have. Namely, peptide ratios may be based on low-abundance peptides or on the signal of each isotopic cluster. Those with a low signal-to-noise ratio may yield skewed results or those with a large difference between the isotope intensities may have saturated signal or fail to detect the lower abundance peak in the pair.²⁴ In Table 2, the results from two complementary experiments are shown for each individual peptide. These data agree fairly well with one another, with errors of approximately 20%, which is on the order of other quantitation methods.²⁴ It is important to point out that our methodology allows quantitation of both the intact protein and the individual peptides after trypsin digestion so that both global and local effects can be seen. The protein ratio was 2:1 oxidized: control while the individual peptides varied from 2:1 to 10:1 with average peptide ratio 4:1.

In Figure 6, the locations of these quantitative results are mapped to the surface of rHSA. Notice that there are three

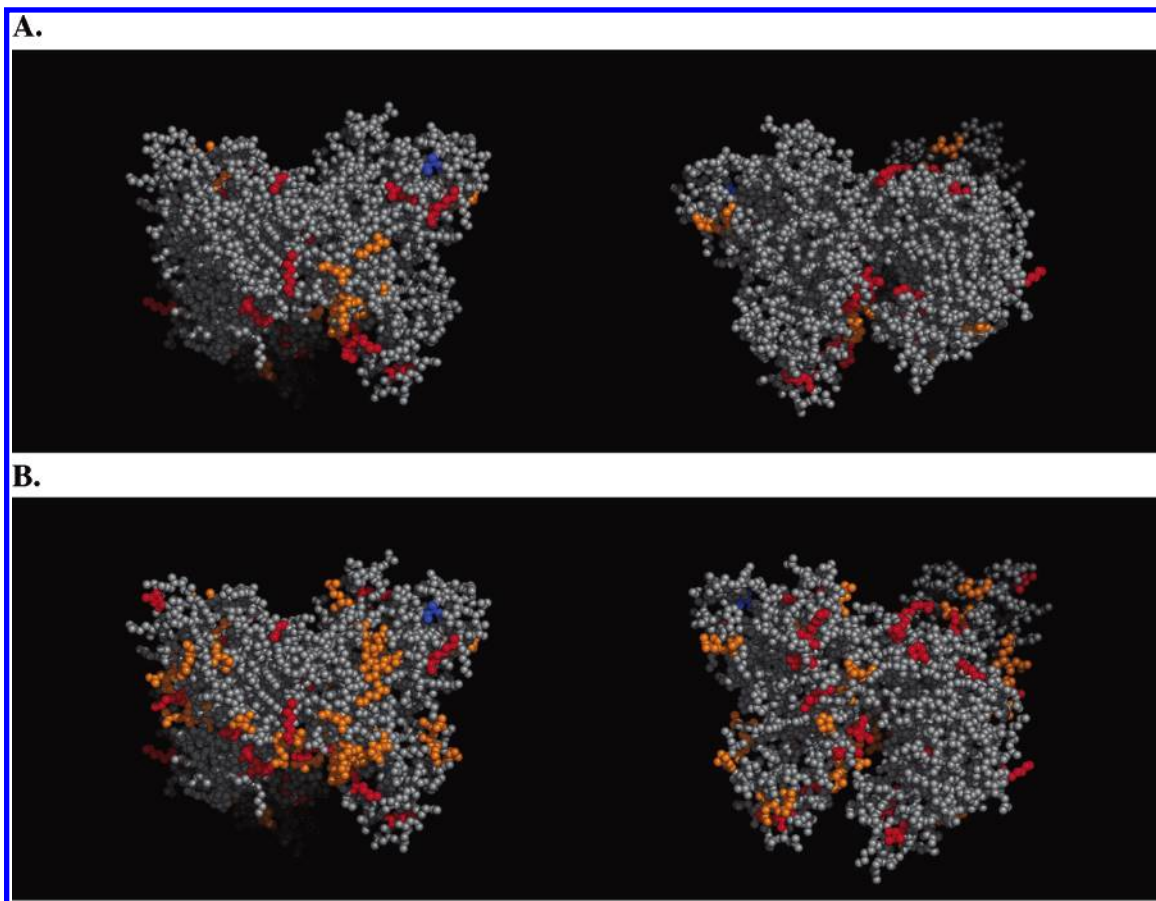


Figure 5. Oxidized and tagged peptides mapped onto the crystal structure of HSA (PDB file: 1A06, www.rcsb.org). The oxidized amino acids are shown in red for definitive candidates and in orange for those peptides with more than one candidate amino acid. The N-terminus, on the front of the protein, is colored in blue for reference. The front view is shown to the left, rotating the protein 180° yields the back view, shown to the right. **A.** rHSA control: peptides identified on the native protein. **B.** FeEDTA/ascorbate-Mediated Oxidation: peptides identified on the FeEDTA/ascorbate oxidized protein.

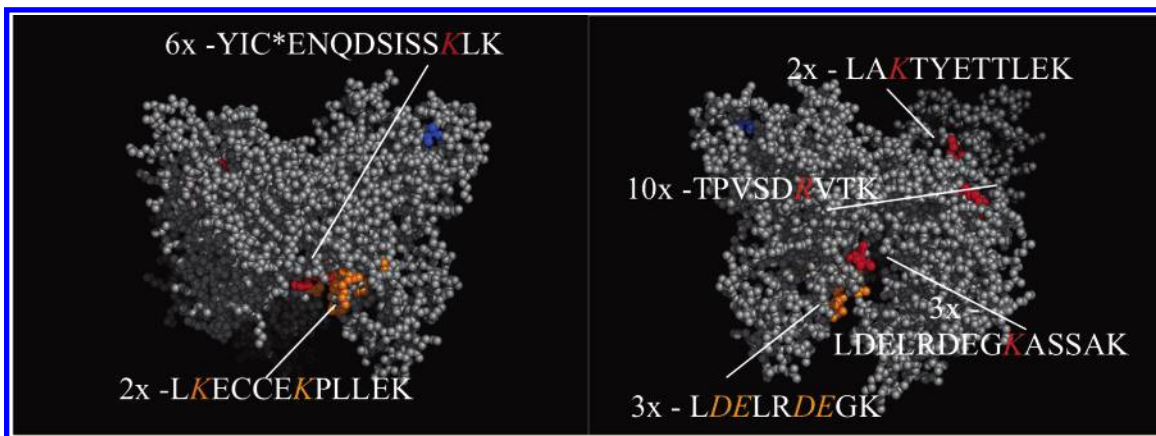


Figure 6. Quantitation data from Table 2 mapped onto the crystal structure of rHSA (PDB file: 1A06, www.rcsb.org). The oxidized amino acids are shown in red for definitive candidates and in orange for those peptides with more than one candidate amino acid. The N-terminus, on the front of the protein, is colored in blue for reference. The front view is shown to the left, rotating the protein 180° yields the back view, shown to the right. The amount of increase seen in the FeEDTA/ascorbate samples over the control samples are indicated for each peptide.

lysine oxidation sites in close proximity in the bottom cleft visible in these views. Interestingly the YIC*ENQDSISSKLLK peptide exhibits a 6-fold increase in oxidation where the other neighboring lysine-containing peptides exhibit only a 2- to 3-fold increase in oxidation. This is despite the less oxidized peptide having two lysine residues available for oxidation. This

and the other variations in site preference detailed above demonstrate the importance of the site-specific oxidation information gained from this methodology. Not only may site-specific oxidation information help in our fundamental understanding of protein oxidation but could potentially serve as site-specific oxidation biomarkers of disease. This may also

Table 2. Relative Quantitation of FeEDTA/Ascorbate-Oxidized rHSA versus rHSA Control, Native Oxidized Peptides^a

peptide	FeEDTA/ native (Tb/Tm)	FeEDTA/ native (Tm/Tb)	FeEDTA/ native (average)
LDEL RDEGK	2.5	3.2	2.9
TPVSDR V TK	11.5	8.0	9.8
LDEL R DEG K ASSAK	1.6	3.5	2.6
L K ECCE K PLLEK	1.6	2.5	2.1
LAKTYET T LEK	2.8	1.7	2.3
YIC [*] ENQDSISS K LK	5.3	5.7	5.5

^a In column 1, the corresponding peptide is identified with the oxidized residues or candidate oxidized residues in bold and carboxymethylation of cysteine indicated with an asterisk. In column 2 integrated intensity ratios of Tb signal to Tm signal where Tb was used in tagging the FeEDTA/ascorbate-oxidized rHSA oxidation sites and Tm was used to tag the control rHSA oxidation sites. In column 3 integrated intensity ratios of Tm signal to Tb signal where Tm was used in tagging the FeEDTA/ascorbate-oxidized rHSA oxidation sites and Tb was used to tag the control rHSA oxidation sites. In column 4 the average of columns 2 and 3 is given.

help elucidate the mechanisms of disease and the role of protein oxidation in oxidation linked diseases.

Conclusions. We have validated the O-ECAT AOD system using the model protein rHSA to show that we can not only detect and quantify aldehyde and ketone groups on oxidized proteins but also identify and quantitate specific oxidized residues on the protein. This methodology represents a significant advancement over existing methods to study protein oxidation. This methodology not only tags oxidized proteins such as DNPH methods, but also can quantitate using isotopes, and achieves site-specificity on more amino acids using high-resolution MS.

All observed oxidation sites mapped to the surface of the protein. Arginine and lysine residues appeared to be more readily oxidized to aldehyde/ketone end products than the other amino acids observed. This is in agreement with the work by Stadtman et al. which showed that oxidized lysine, arginine, and proline residues are the major products of metal-catalyzed oxidation.⁷ The quantitative results exhibited oxidation site preference that appeared independent of the oxidized residue. We expect that this general methodology can be extended to study disease-related oxidation. Given the site specificity observed here we expect that the site-specific information this method provides will be useful in understanding the biochemical mechanisms of such diseases. In the process of such studies, diagnostic site-specific oxidation biomarkers may also be found. We are currently extending method to study protein-protein interactions using the tethered iron chelate FeBABA to oxidatively tag protein binding partners. Further exploration on the use of the multiplexing of M-AOD, using up to 7 monoisotopic metals, is also planned.

Abbreviations. O-ECAT, oxidation-dependent carbonyl-specific Element-Coded Affinity Mass Tag; DOTA, 1,4,7,10-tetraazacyclododecane-*N,N',N'',N'''*-tetraacetic acid; AOD, ((*S*)-2-(4-(2-aminoxy)-acetamido)-benzyl)-DOTA.; M, rare earth element; rHSA, recombinant human serum albumin; nanoLC-FTICR-MS, nanoliquid chromatography-Fourier transform ion cyclotron resonance-mass spectrometry; DNPH, 2,4-dinitrophenylhydrazine; FeEDTA, iron (III) ethylenediaminetetraacetic acid; ABD-*t*Bu₄, (*S*)-2-(4-aminobenzyl)-DOTA tetra-tertbutyl ester, DIPCDI, diisopropylcarbodiimide; DMF, *N,N*-dimethylformamide; TBS, 24.8mM Tris, 137mM NaCl, 0.269mM KCl, pH 7.4; TBST, TBS with 0.05% (v/v) Tween-20; AP, alkaline phosphatase; HSA, human serum albumin; MS, mass spec-

trometry; NBD, (*S*)-2-(4-nitrobenzyl)-DOTA.; TEOAc, triethylammonium acetate.

Acknowledgment. We thank Mark Scalf and Yi-Hwa Hwang for their help in the development of the work. We thank Laurel Beckett and Judy Li for helpful discussions and statistical analysis of the data. We thank Gary Kruppa for providing elements of the data analysis software. We also thank Mark McCoy for assistance with data processing. This work was supported by National Institutes of Health research Grant Nos. GM25909 to C.F.M. and GM049077 to C.B.L. and the Department of Energy Advanced Study Program to N.L.Y. Portions of this work were performed under the auspices of the U.S. Department of Energy by University of California, Lawrence Livermore National Laboratory under Contract W-7405-Eng-48.

References

- Dalle-Donne, I.; Giustarini, D.; Colombo, R.; Rossi, R.; Milzani, A. *Trends Mol. Med.* **2003**, *9*, 169–176.
- Butterfield, D. A. *Brain Res.* **2004**, *1000*, 1–7.
- Levine, R. L. *Free Radical Biol. Med.* **2002**, *32*, 790–796.
- Mary, J.; Vouquier, S.; Picot, C. R.; Perichon, M.; Petropoulos, I.; Friguet, B. *Exp. Gerontol.* **2004**, *39*, 1117–1123.
- Xu, G. Z.; Takamoto, K.; Chance, M. R. *Anal. Chem.* **2003**, *75*, 6995–7007.
- Xu, G. Z.; Chance, M. R. *Anal. Chem.* **2004**, *76*, 1213–1221.
- Requena, J. R.; Chao, C.-C.; Levine, R. L.; Stadtman, E. R. *PNAS* **2001**, *98*, 69–74.
- Meade, S. J.; Miller, A. G.; Gerrard, J. A. *Bioorg. Med. Chem.* **2003**, *11*, 853–862.
- Robinson, C. E.; Keshavarzian, A.; Pasco, D. S.; Frommel, T. O.; Winship, D. H.; Holmes, E. W. *Anal. Biochem.* **1999**, *266*, 48–57.
- Fagan, J. M.; Slecza, B. G.; Sohar, I. *Int. Jo. Biochem. Cell Biol.* **1999**, *31*, 751–757.
- Sharp, J. S.; Becker, J. M.; Hettich, R. L. *Anal. Chem.* **2004**, *76*, 672–683.
- Davies, M. J.; Fu, S. L.; Wang, H. J.; Dean, R. T. *Free Radical Biol. Med.* **1999**, *27*, 1151–1163.
- Anderson, L. B.; Ouellette, A. J. A.; Eaton-Rye, J.; Maderia, M.; MacCoss, M. J.; Yates, J. R.; Barry, B. A. *J. Am. Chem. Soc.* **2004**, *126*, 8399–8405.
- Mirzaei, H.; Regnier, F. *Anal. Chem.* **2005**, *77*, 2386–2392.
- Yoo, Y. S.; Regnier, F. E. *Electrophoresis* **2004**, *25*, 1334–1341.
- Hall, M. P.; Ashrafi, S.; Obegi, I.; Petesch, R.; Peterson, J. N.; Schneider, L. V. *J. Mass Spectrom.* **2003**, *38*, 809–816.
- Whetstone, P. A.; Butlin, N. G.; Corneillie, T. M.; Meares, C. F. *Bioconjugate Chem.* **2004**, *15*, 3–6.
- Corneillie, T. M.; Lee, K. C.; Whetstone, P. A.; Wong, J. P.; Meares, C. F. *Bioconjugate Chem.* **2004**, *15*, 1392–1402.
- Corneillie, T. M.; Whetstone, P. A.; Fisher, A. J.; Meares, C. F. *J. Am. Chem. Soc.* **2003**, *125*, 3436–3437.
- Sugio, S.; Kashima, A.; Mochizuki, S.; Noda, M.; Kobayashi, K. *Protein Eng.* **1999**, *12*, 439–446.
- Moi, M.; Meares, C. F.; DeNardo, S. J. *J. Am. Chem. Soc.* **1988**, *110*, 6266–6267.
- Corson, D. T.; Meares, C. F. *Bioconjugate Chem.* **2000**, *11*, 292–299.
- Takenouchi, K.; Tabe, M.; Watanabe, K.; Hazato, A.; Kato, Y.; Shionoya, M.; Koike, T.; Kimura, E. *J. Org. Chem.* **1993**, *58*, 6895–6899.
- Ong, S.-E.; Kratchmarova, I.; Mann, M. *J. Proteome Res.* **2003**, *2*, 173–181.
- Taborsky, G. *Biochemistry* **1973**, *12*, 1341–1348.
- Choi, J.; Malakowsky, C. A.; Talent, J. M.; Conrad, C. C.; Carroll, C. A.; Weintraub, S. T.; Gracy, R. W. *Biochim. Biophys. Acta (BBA) – Mol. Basis Dis.* **2003**, *1637*, 135–141.
- Choi, J.; Conrad, C. C.; Dai, R.; Malakowsky, C. A.; Talent, J. M.; Carroll, C. A.; Weintraub, S. T.; Gracy, R. W. *Proteomics* **2003**, *3*, 73–77.
- Sokolowska, M.; Krezel, A.; Dyba, M.; Szweczek, Z.; Bal, W. *Eur. J. Biochem.* **2002**, *269*, 1323–1331.

PR050299Q